J. Fluid Mech. (1982), *vol.* 115, *pp.* 151–164
Printed in Great Britain

A contribution to the free-stream turbulence effect on the flow past a circular cylinder

BY MASARU KIYA†, YASUHIRO SUZUKI, MIKIO ARIE AND MITSUTOSHI HAGINO

Faculty of Engineering, Hokkaido University, Sapporo, 060, Japan

(Received 19 June 1980 and in revised form 8 July 1981)

The effect of the free-stream turbulence on the flow past a circular cylinder was studied experimentally in the subcritical and critical regimes. Several grids were used to produce approximately homogeneous turbulent fields with longitudinal integral scales ranging from 0·30 to 3·65 cylinder diameters and with the longitudinal intensities ranging from 1·4 to 18·5 %.

The critical Reynolds number R_c at which the time-mean drag coefficient obtains the value of 0·8 was found to satisfy the relation $R_c^{1\cdot34}T = 1\cdot98 \times 10^5$, where T is the Taylor number defined in terms of the longitudinal integral scale. The time-mean drag coefficient, the base-pressure coefficient and the spanwise correlation length of the surface-pressure fluctuations in the vicinity of the separation point were fairly well correlated with the parameter $R^{1\cdot34}T$, R being the Reynolds number. It was argued that the parameter $R^{1\cdot34}T$ will control some aspects of the flow past a circular cylinder immersed in turbulent streams.

1. Introduction

The effect of the free-stream turbulence on the properties of flow around a rigid circular cylinder has been studied experimentally by many investigators: Fage & Warsap (1929), Bearman (1968), Morishita & Nomura (1968), Surry (1972), Ko & Graf (1972), Batham (1973), Bruun & Davies (1975), Modi & El-Sherbiny (1977). These authors are concerned with circular cylinders immersed in nearly homogeneous turbulent flows generated by grids. The grid-generated turbulent flows can be characterized by the intensity $(\overline{u^2})^{\frac{1}{2}}/U_\infty$ (U_∞ = time-mean free-stream velocity) and the longitudinal integral scale L_x of the streamwise component u of the velocity fluctuation. The flow past a circular cylinder depends not only on the intensity and scale of the free-stream turbulence but on the Reynolds number $R = U_\infty d/\nu$, where d is the diameter of the cylinder and ν denotes the kinematic viscosity.

For bluff bodies with salient edges, the flow around them is sensibly independent on the Reynolds number, so that their aerodynamic properties such as the drag coefficient and the base-pressure coefficient can be described as functions of the intensity and the scale. On the assumption that the principal effect of the external turbulent flow is the extra entrainment of fluid out of the wake, Bearman (1971) introduces the turbulence parameter

$$T_1 = [(\overline{u^2})^{\frac{1}{2}}/U_\infty](L_x^2/A), \tag{1}$$

† Present address: Department of Applied Mathematics and Theoretical Physics, University of Cambridge, England.

for square plates, where A is the area of the plate. He shows that the base-pressure coefficient is well-correlated with this parameter. Following a slightly different approach, Humphries & Vincent (1976) obtain another turbulence parameter

$$T_2 = l_f k_f^{\frac{1}{2}}/(U_\infty h), \tag{2}$$

for the square, circular and triangular plates. Here l_f and k_f are respectively the length and the kinetic energy per unit mass of the free-stream turbulence, and h is a representative length of the bodies. They argue that the parameter T_2 uniquely controls the base-pressure and the separation-bubble length of the bodies. For homogeneous turbulence, T_2 can be reduced to

$$T_2^* = [(\overline{u^2})^{\frac{1}{2}}/U_\infty](L_x/h). \tag{3}$$

The fact that the parameters T_1 and T_2^* are not equivalent, although they are individually well-correlated with the base-pressure coefficient, has not yet been explained.

For circular cylinders, Bearman (1968) shows that the critical Reynolds number R_c at which the drag coefficient C_D obtains some predetermined value is a function of the Taylor number T_y, i.e.

$$T_y = [(\overline{u^2})^{\frac{1}{2}}/U_\infty](d/L_y)^{\frac{1}{5}}, \tag{4}$$

where L_y is the lateral integral scale of the free-stream turbulence. In homogeneous turbulence L_y is equal to $\frac{1}{2}L_x$. The value $C_D = 0{\cdot}8$ is chosen by Bearman (1968) as a representative value for circular cylinders. Although several values of R_c plotted against T_y (Bearman 1968, figure 11) seem to collapse onto one single curve, the scarcity of the data prevents the determination of a definite functional relation between R_c and T_y. (Bruun & Davies (1975) represent R_c as a linear function of T_y in the range $4 \times 10^4 \leqq R_c \leqq 1{\cdot}2 \times 10^5$ on the basis of Bearman's (1968) result. As will be shown in § 3, however, the linear relation was inappropriate in view of the data compiled by the present authors.) Ko & Graf (1972) argue that, in a Reynolds-number range $1350 \leqq R \leqq 8000$, the drag coefficient of a circular cylinder is collapsed onto a single curve when plotted against the parameter

$$T_3 = T/\log R, \tag{5}$$

where T is the Taylor number defined in terms of L_x, i.e.

$$T = [(\overline{u^2})^{\frac{1}{2}}/U_\infty](d/L_x)^{\frac{1}{5}}. \tag{6}$$

The parameter T_3 seems to be inappropriate in the range $R > 10^4$.

The purpose of this paper is to study the effect of the free-stream turbulence on the flow past a circular cylinder in the subcritical and critical Reynolds-number regimes, and thereby to find a certain combination of the turbulence parameters and the Reynolds number with which some important aerodynamic properties of a circular cylinder are correlated with reasonable accuracy. Since the Reynolds-number range tested in this experiment was limited, data from various sources were employed to serve this purpose.

2. Experimental apparatus and method

The experiments were performed in an open-return, low-speed air tunnel with a 35 cm by 35 cm, 120 cm long working section. Highly turbulent flows were generated by the installation of square-mesh grids at the beginning of the working section. The grids

were constructed of bars of rectangular or circular cross-section. With the grids in position, the velocity of the air flow in the tunnel was in the range 11·0–15·4 m/s.

Circular cylinders tested were smoothly machined brass and their diameters ranged from 0·955 to 5·03 cm. The cylinders were mounted separately, normal to the flow and spanning the tunnel. The aspect ratio of the cylinders thus ranged from 6·89 to 36·6 and the tunnel-wall blockage ratio from 0·027 to 0·145. A pressure tap of 0·6 mm diameter was provided at the mid-span position of each cylinder and allowed the time-mean pressure distribution along the cylinder surface to be obtained by the rotation about its axis. The time-mean pressure was read on a Betz manometer or a differential-transformer type of pressure transducer, whose output was integrated during 60 s to obtain the time-mean value.

Another cylinder of 3·18 cm diameter was prepared to measure the surface-pressure fluctuations. The cylinder was cut into two parts at its mid-span position. First, each part was provided near its end with a pressure tap of 0·8 mm diameter connected to a semiconductor strain-gauged transducer, with a small cavity between the cylinder surface and the diaphragm of the transducer. Spacers of various lengths were inserted separately between the two parts in such a manner that the pressure taps were at the same angle from the front stagnation point. The minimum distance between the pressure taps was 0·094 times the diameter. In this mode, the model allowed the determination of the spanwise correlation length of the pressure fluctuations at arbitrary angles from the front stagnation point. Secondly, the two parts were combined by a circular segment of the same diameter which had two pressure taps of 0·8 mm diameter at the same spanwise position, where they were separated by 180°. The pressure taps were connected to the aforementioned pressure transducers in exactly the same way as in the first case. The rotation of the cylinder about its axis allowed the measurement of the cross-correlation of pressure fluctuations at two opposing points on the cylinder surface and the difference between them, which may yield an estimate of the fluctuating lift force acting on the cylinder.

The pressure transducers responded to the pressure fluctuations up to 150–200 Hz with a gain factor of $1 \pm 0{\cdot}06$ with negligible phase lag. These frequencies were well above the frequencies of vortex shedding from the cylinder.

The velocity fluctuation in the flow field was detected by linearized constant-temperature hot-wire anemometers (KANOMAX 2700). The outputs of the hot-wire anemometers and the pressure transducers were recorded on an analogue tape recorder (KYOWA R-520A) and were later analysed on a digital correlator (SAICOR 42A) or a digital signal processor (SANEI 7T07A) to obtain their autocorrelations, cross-correlations and power-spectral densities. An analogue low-pass filter (1 KHz) was placed between the hot-wire and pressure-transducer outputs and the data-processing equipment to avoid aliasing error. The root-mean-square values of the velocity and pressure fluctuations were obtained by a true r.m.s. meter.

3. Experimental results and discussion

Flow behind turbulence-producing grids

The grids produced approximately homogeneous turbulence with the range of the intensity $(\overline{u^2})^{\frac{1}{2}}/U_\infty$ and the integral scale summarized in table 1 at downstream distances X from the grids corresponding to the cylinder locations used for most measure-

Grid	M (cm)	b (cm)	X (cm)	$(\overline{u^2})^{\frac{1}{2}}/U_\infty$	L_x (cm)
1	3·3	1·1	30	0·119	1·52
2	4·5	1·5	30	0·185	2·22
—	—	—	60	0·106	3·49
3	9·0	2·5	60	0·128	2·52

TABLE 1. Intensity and longitudinal integral scale of grid-generated turbulent flows. Grids consisted of square rods of side b. M is the mesh size of the grids.

ments reported in the following sections. The integral scale L_x was evaluated as the product of the mean velocity U_∞ and the integral time scale of the longitudinal velocity component. The X-probe measurements showed that the turbulence energy was approximately equally distributed among its three components.

At the locations shown in table 1, the mean velocity and the intensity of turbulence were found to be uniform to within $\pm$ 3 % over the area to be occupied by the cylinders. Moreover, at a fixed distance from the grids, the intensity and scale changed only slightly with increased mean velocity.

Since the minimum value of X/M, M being the mesh size, was 6·7 in the present experiment, one may naturally suspect whether the turbulent field was affected by shadows of bars and had significant inhomogeneities in the direction normal to the mean flow. It is shown, however, that if the upwind turbulence is restricted to a narrow region of about $2L_x$ on either side of the stagnation line, then the effect on the wake of bluff bodies is the same as if the upwind turbulence was homogeneous with the same intensity and scale (Durbin & Hunt 1979). Accordingly, the short distance between the grids and the cylinders will not present serious difficulties in studying the effects of the upwind turbulence.

Tunnel-wall blockage corrections

The tunnel-wall blockage ratio amounted to 14·5 % at its maximum, so that the measured data should be corrected for the effects of blockage. Since the drag coefficient and thus the flow conditions around the cylinders were changing rapidly with the Reynolds number, it is doubtful whether any correction method can completely compensate for the blockage effects. As cogently remarked by Roshko (1961) and Bearman (1968), the method of Allen & Vincenti (1944) should be regarded as the most appropriate to use over the Reynolds-number range examined and was therefore employed throughout this work.

This method gives the corrected values of the free-stream velocity U_∞ and the drag coefficient C_D in terms of the measured value and the blockage ratio. It has been assumed that the corrections for the Reynolds number R and the inverse of the Strouhal number S ($= fd/U_\infty$, f being the vortex-shedding frequency) are the same as for the velocity. A formula for the correction of the measured pressure distribution is given in Roshko (1961).

In the present work, the uncorrected drag coefficient was obtained by integrating the measured pressure distribution: corrected values of the relevant quantities were then calculated. The maximum corrections to the free-stream velocity and the drag coefficient were 3·6 and 10·2 %, respectively. The fluctuating quantities were not corrected for the blockage effect.

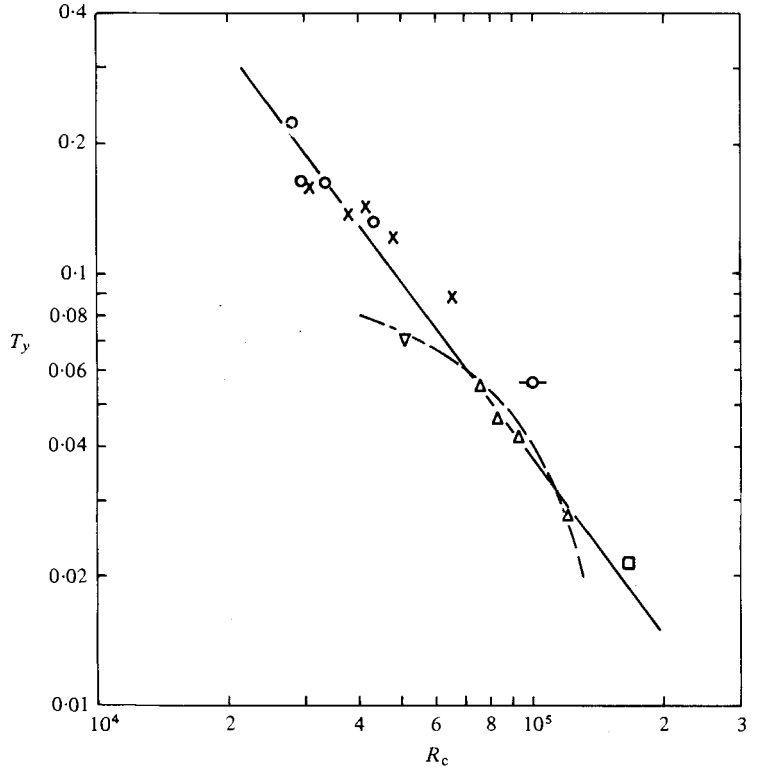

FIGURE 1. Relation between Taylor number T_y and critical Reynolds number R_c at which the time-mean drag coefficient C_D obtains the value of 0·8. ○, present results; △, Fage & Warsap (1929) as compiled by Bearman (1968); ▽, Bearman (1968); ×, Modi & El-Sherbiny (1977); □, Sakata (1981); —○—, Bruun & Davies (1975); ——, best-fit straight line; – · –, empirical formula of Bruun & Davies (1975).

Drag, base pressure and Strouhal number

In accordance with the results of previous investigators, the fall in the measured drag coefficient through the critical regime occurred at a lower Reynolds number in the turbulent flows than in smooth flows, and thus the C_D versus R curve generally shifted to the side of low Reynolds number. Bearman (1968) shows that the onset of the critical regime can be correlated with the Taylor number T_y, which is derived by hypothesizing that the boundary-layer transition is controlled by pressure-gradient variations due to the free-stream turbulence. The critical Reynolds number R_c is defined as the Reynolds number at which the drag coefficient has a value of 0·8 (Bearman 1968). The critical Reynolds numbers thus determined are plotted in figure 1 against T_y, together with the data from several sources. The lateral length scale L_y in the Taylor number was assumed to be $\frac{1}{2}L_x$ when L_y was not measured. The relation $L_y = \frac{1}{2}L_x$ is exact for homogeneous turbulence and was also a reasonable approximation in the turbulent flows employed in this work.

The present data, Sakata's (1981) result and the data compiled by Bearman (1968) collapsed fairly well onto a straight line whose gradient was found to be $-1{\cdot}34$ by the least-squares method. The data of Bruun & Davies (1975) and Modi & El-Sherbiny (1977) were not included to obtain the best-fit straight line because the authors took

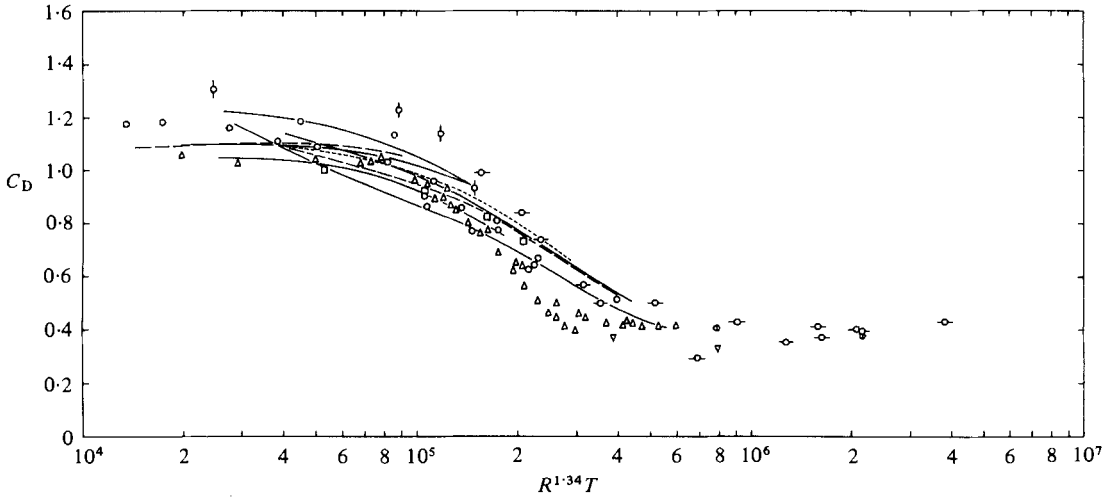

FIGURE 2. Time-mean drag coefficient C_D plotted against the parameter $R^{1·34}T$. ○, present results; △, Fage & Warsap (1929); ▽, Bearman (1968); ⊖, Surry (1972); ●, Batham (1973); -○-, Bruun & Davies (1975); □, Sakata (1981); solid and broken lines for Modi & El-Sherbiny (1977).

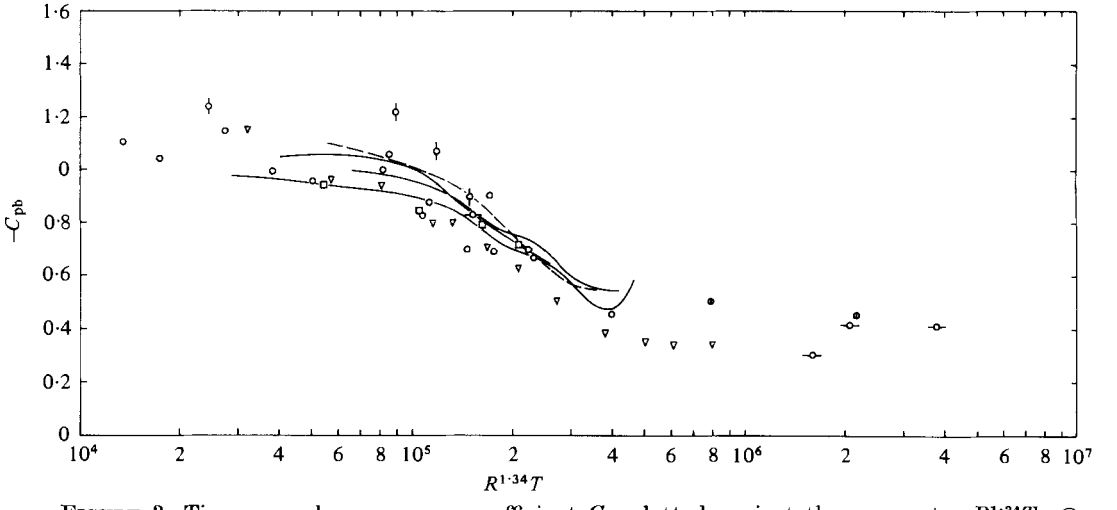

FIGURE 3. Time-mean base-pressure coefficient C_{pb} plotted against the parameter $R^{1·34}T$. ○, present results; ▽, Bearman (1968); ⊖, Surry (1972); ●, Batham (1973); -○-, Bruun & Davies (1975); □, Sakata (1981); solid and broken lines for Modi & El-Sherbiny (1977).

the liberty of assuming in their results that the turbulence intensity and scale at the critical Reynolds number were the same as those at another Reynolds number. R_c and T_y are then related by

$$T_y R_c^{1·34} = 1·72 \times 10^5, \tag{7}$$

which will hold in the range $3 \times 10^4 < R_c < 1·5 \times 10^5$. Since the C_D versus R curves for various free-stream turbulence were roughly parallel in the critical regime, the drag coefficient plotted against a new parameter $R^{1·34}T$ will be expected to collapse into a narrow region. Figure 2 demonstrates that this is the case.

The base-pressure coefficient C_{pb} is plotted in figure 3 against $R^{1·34}T$, together with

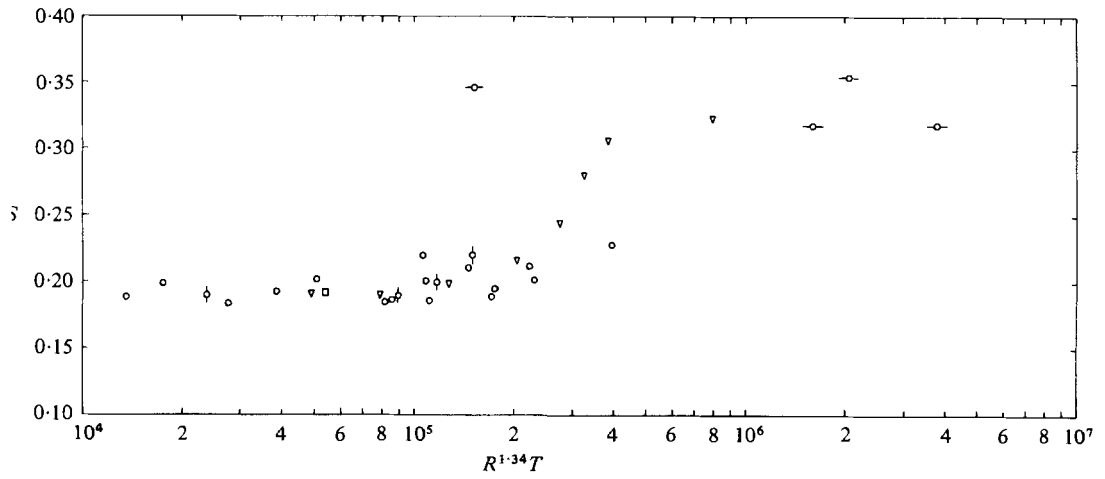

FIGURE 4. Strouhal number of vortex shedding S plotted against the parameter $R^{1\cdot34}T$. ○, present results; ▽, Bearman (1968); ◇, Surry (1972); -○-, Bruun & Davies (1975); □, Sakata (1981).

the results of several investigators. The correlation between $R^{1\cdot34}T$ and C_{pb} may be thought of as reasonable, except for the data of Surry (1972), which seem to be too low.

Figure 4 presents the Strouhal number as a function of the parameter $R^{1\cdot34}T$. The data point furthest to the left of Bruun & Davies (1975) taken at $R = 8{\cdot}0 \times 10^4$ should be taken with reserve, because it implies an unusually high value of the Strouhal number as compared with that in the subcritical regime. Since the Strouhal number in the subcritical regime shows a relatively small change with the Reynolds number and the free-stream turbulence, the appropriateness of the parameter $R^{1\cdot34}T$ should be examined in the critical regime. The data in the critical regime, however, for which the free-stream turbulence intensity and scale are specified are scarce, so that it is not clear at present whether this parameter can collapse the Strouhal number onto a single curve with tolerable accuracy.

According to Gerrard (1965), the Strouhal number behaves like a mean rather than an oscillating quantity because the strengths of the vortices depend most strongly upon the mean rate of shedding of vorticity, which is governed by the behaviour of the separated shear layers. Accordingly it may not be necessarily unreasonable to expect that the Strouhal number in the critical regime will be correlated with the parameter $R^{1\cdot34}T$.

From the above results, it is likely that the parameter $R^{1\cdot34}T$ approximately controls a few properties of the flow around a circular cylinder in turbulent free streams. This implies that the effect of the free-stream turbulence on *some* properties of the flow may be interpreted as an effective increase in the Reynolds number. Although a few authors (e.g. Bearman 1980) cast a serious doubt on this interpretation, the present authors are nevertheless of the opinion that this should not necessarily be rejected for a few aspects of the flow concerned. The effect of the free-stream turbulence will modify not only the behaviour of the boundary layer along the cylinder surface but also that of the fully separated shear layers. The Taylor number is originally derived as a criterion for the boundary-layer transition due to the free-stream turbulence (Taylor 1936), so that it has no direct connection with the behaviour of the separated

Case	$(\overline{u^2})^{\frac{1}{2}}/U_\infty$	L_x/d	R	T	$R^{1\cdot34}T$	C_D	S
1	0·014	—	$3\cdot16\times10^4$	—	—	1·20	0·20
2	0·029	0·48	$3\cdot98\times10^4$	0·0336	$4\cdot56\times10^4$	1·15	0·20
3	0·064	0·79	$2\cdot65\times10^4$	0·0671	$5\cdot30\times10^4$	1·15	0·20
4	0·106	1·09	$2\cdot72\times10^4$	0·104	$8\cdot52\times10^4$	1·14	0·19
5	0·128	0·79	$2\cdot64\times10^4$	0·134	$1\cdot06\times10^5$	0·91	0·21
Surry (1972)	0·147	4·4	$3\cdot38\times10^4$	0·109	$1\cdot19\times10^5$	1·14	0·20

TABLE 2. Parameters of the flow past a circular cylinder employed in surface-pressure measurements

shear layers. If the nature of the boundary layer, however, is assumed to impose a strong initial condition on the shear layers, it is possible that the Taylor number may behave as a governing parameter also for the shear layers. The extent to which the free-stream turbulence is effective in determining the nature of the boundary layer and the separated shear layers will depend on the Reynolds number. The above discussion seems to lend support to the employment of a parameter such as $R^{1\cdot34}T$ to correlate some aerodynamic properties of a circular cylinder with the free-stream turbulence. It was conjectured that cases of extremely low free-stream turbulence will not be included in the present correlations. Moreover, the Reynolds number should be in the range $10^4 < R < 10^6$.

Surface-pressure fluctuations

The results to be described here were obtained for a circular cylinder of 3·18 cm diameter. The relevant experimental conditions are summarized in table 2. It may be noted that the parameter $R^{1\cdot34}T$ increased from case 2 to case 5, in this order, and that the flow past the cylinder was in the subcritical regime, i.e. $C_D > 0\cdot8$. For case 1, it was difficult to obtain the integral time scale of the longitudinal turbulent-velocity component from which the longitudinal integral scale was to be calculated, because the autocorrelation curve decayed very slowly with increasing time delay.

The time-mean and r.m.s. values of surface-pressure fluctuations are presented in figures 5 and 6 as functions of the angle θ which is measured from the leading generator. Also plotted in figure 6 are the shedding peaks of the pressure spectrum $(E_p)_{peak}$, where E_p is defined by

$$\int_0^\infty E_p(f)\,df = p'^2. \tag{8}$$

Here f is the frequency and p' denotes the r.m.s. value of the fluctuating component of the surface pressure p, i.e. $p' = (\overline{p^2})^{\frac{1}{2}}$. In the vicinity of the position $\theta = 180°$, a spectral peak appeared at the frequency which was twice the Strouhal frequency.

For all cases other than case 5, primary peaks of p' and $(E_p)_{peak}$ appeared at the position $\theta \simeq 75°$, which was supposed to be a little upstream of the separation point, and the peak values of p' were approximately the same. For case 5, where the free-stream turbulence intensity was the highest, the peak in the r.m.s. pressures shifted rearward (probably corresponding to the movement of the separation point) and its value amounted to as much as 50 % of the dynamic pressure of the free stream. It seems in case 5 that a broad maximum of $(E_p)_{peak}$ occurred at $\theta \simeq 90°$, which was approximately 15° upstream of the position where the peak of p' appeared.

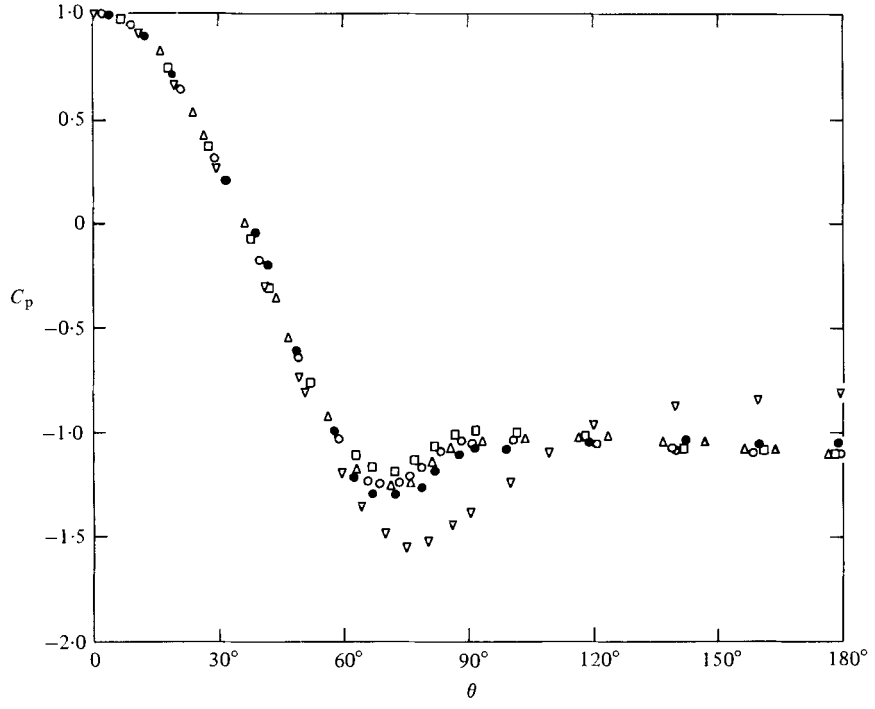

FIGURE 5. Time-mean pressure distribution on the cylinder surface. C_p = time-mean pressure divided by $\frac{1}{2}\rho U_\infty^2$. □, case 1; ○, case 2; △, case 3; ●, case 4; ▽, case 5. Cases 1–5 are defined in table 1.

The general level of $(E_p)_{peak}$ decreased with increasing intensity of the free-stream turbulence, whereas the levels of the r.m.s. pressures in the region downstream of the separation point were relatively independent of the turbulence intensity. The values of $(E_p)_{peak}$ decreased sharply towards the rear stagnation point despite the fact that the r.m.s. pressures remained unchanged there, especially when the turbulence intensity was low. This feature implies that the high levels of the r.m.s. pressures in the wake region were contributed mainly by broad-band fluctuations there.

For case 4, there was a drop in the r.m.s. pressures from the front stagnation point. This is believed to be associated with the distortion of the free-stream turbulence near the circular cylinder (Durbin & Hunt 1980).

The spanwise correlation length L_{pz} of the surface-pressure fluctuations plotted against the angle θ was found to change only slightly over a range $30° < \theta < 150°$. It should be noted that the pressure fluctuations over all the frequencies below 200 Hz (which was about 2·0 times the maximum vortex-shedding frequency in this experiment) were included in the calculation of L_{pz}. The correlation length along the generator $\theta = 90°$ is plotted as a function of the parameter $R^{1\cdot34}T$ in figure 7, which shows that the data from several sources collapsed fairly well onto a single curve.

If it is assumed that the fluctuating lift experienced by a circular cylinder is dependent primarily on the pressure fluctuations in the vicinity of $\theta = 90°$ and 270°, its r.m.s. value can be roughly estimated from

$$C'_L \simeq 1\cdot41 \frac{p'_1}{\frac{1}{2}\rho U_\infty^2}(1 - C_{p_1 p_2})^{\frac{1}{2}}. \tag{9}$$

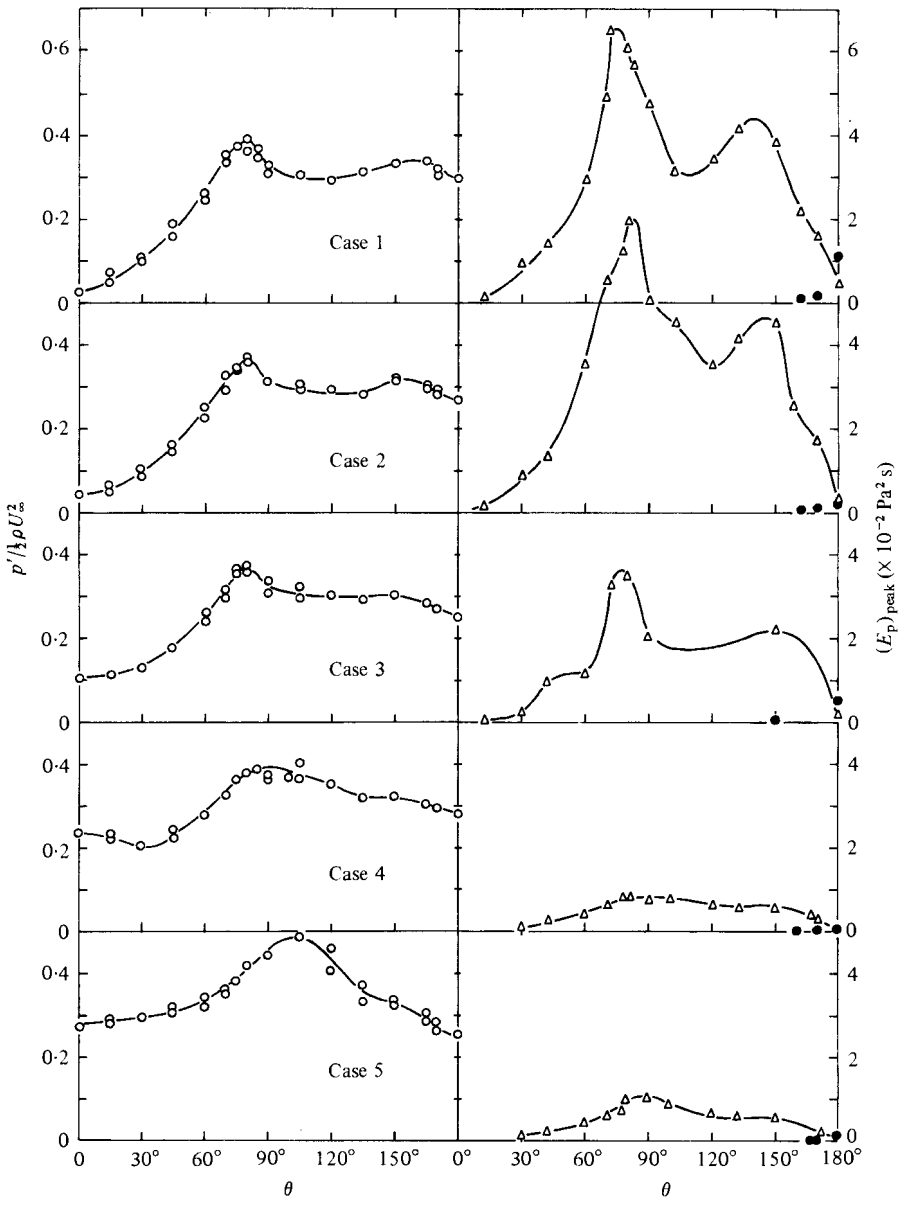

FIGURE 6. The r.m.s. surface-pressure fluctuations p' (on the left) and the spectral peak of the pressure fluctuations $(E_p)_{peak}$ (on the right) plotted against the angle θ. ○, $p'/\frac{1}{2}\rho U_\infty^2$; △, spectral peak at the vortex-shedding frequency f_K; ●, spectral peak at the frequency $2f_K$. ρ = density of fluid. Lines for visual aid only.

Here C'_L is the r.m.s. value of the fluctuating lift divided by $\frac{1}{2}\rho U_\infty^2 d$, p'_1 the r.m.s. pressure at $\theta = 90°$ or 270° and $C_{p_1p_2}$ denotes the cross-correlation coefficient of the surface-pressure fluctuations at $\theta = 90°$ and 270°. A derivation of (9) is given in the appendix. The r.m.s. lift coefficient obtained from (9) ranged from 0·48 to 0·66, thus being well within the scatter of previous experimental data taken in the subcritical regime. Accordingly the fluctuating lift was still dominated by the broad-band Strouhal peak, even in turbulent free-streams of the present experiment.

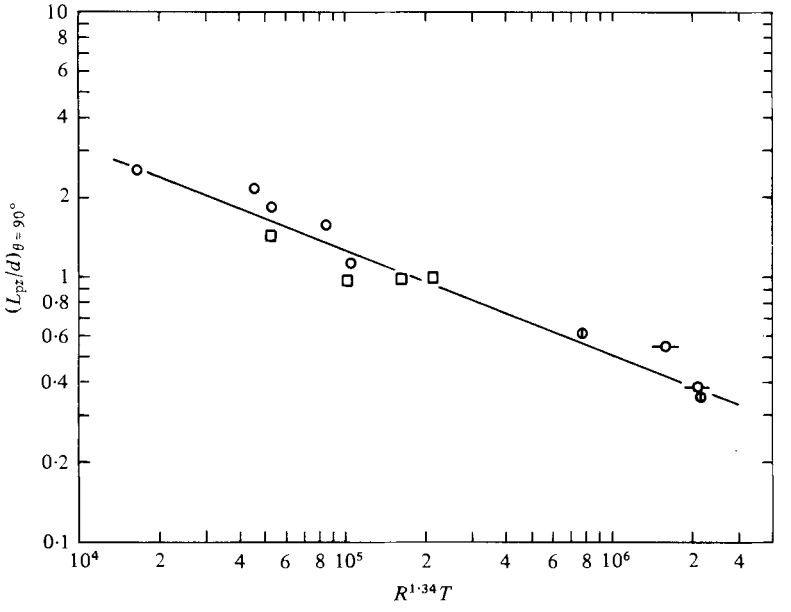

FIGURE 7. Spanwise correlation length of surface-pressure fluctuations at $\theta = 90°$ plotted against the parameter $R^{1·34}T$. ○, present results; ⊕, Batham (1973); -○-, Bruun & Davies (1975); □, Sakata (1981); solid lines for visual aid only.

The cross-correlations of the surface-pressure fluctuations at two points separated by 180° will give a clue to understanding the extent to which the periodic pressure fluctuations associated with the vortex shedding are contaminated by the free-stream turbulence. Let p_1 and p_2 denote the fluctuating components of the surface pressures at two opposing points and α the angle measured from the free-stream direction to the diametral line connecting the two points. Figure 8 shows the correlation coefficient

$$C_{p_1p_2} = \overline{p_1 p_2}/(p_1' p_2') \tag{10}$$

as a function of α. The coefficient $C_{p_1p_2}$ was negative and fairly constant in a range $30° < \alpha < 90°$. The negative correlation was brought about by the periodically alternative vortex shedding from the cylinder. The absolute value of the correlation coefficient decreased with increased turbulence intensity of the free stream.

4. Conclusion

The effect of the free-stream turbulence on a few aerodynamic properties of a circular cylinder has been examined in the subcritical and critical regimes. The main results may be summarized as follows.

(i) The critical Reynolds number R_c at which the time-mean drag coefficient has the value of 0·8 was shown to be fairly well correlated with the Taylor number T_y in the form

$$T_y R_c^{1·34} = 1·72 \times 10^5,$$

where T_y is defined in terms of the lateral integral scale of the free-stream turbulence.

(ii) The time-mean drag coefficient collapsed into a narrow region when plotted against the parameter $R^{1·34}T$, where R is the Reynolds number and T denotes the Taylor number based on the longitudinal integral scale. The base-pressure coefficient

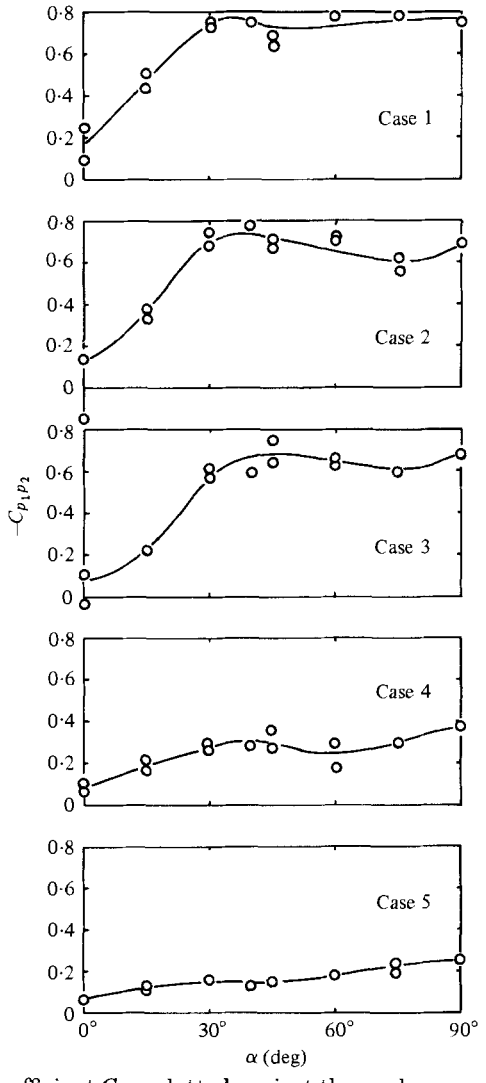

FIGURE 8. Correlation coefficient $C_{p_1p_2}$ plotted against the angle α measured from the free-stream direction to the diametral line connecting the two opposing pressure taps. Lines for visual aid only.

and the spanwise correlation length of the surface-pressure fluctuations at the angle 90° from the leading generator were fairly well correlated with this parameter. It is doubtful, however, whether the parameter $R^{1\cdot34}T$ uniquely controls all the aspects of the flow past a circular cylinder immersed in turbulent streams.

(iii) An approximate formula for the evaluation of the r.m.s. lift coefficient was obtained in terms of the surface-pressure fluctuations at the points $\theta = 90°$ and 270°. This formula was shown to be tolerably accurate.

This research was supported by the Grant-in-Aid for Scientific Research from the Ministry of Education, Science and Culture of Japan. The authors express their sincere thanks to Mr T. Yamazaki and Mr T. Sampo for their assistance in the construction of the experimental apparatus.

Appendix. Derivation of (9)

It was assumed that the r.m.s. lift fluctuation is governed primarily by the pressure fluctuations in the vicinity of $\theta = 90°$ and 270°. The mean-square value of the lift fluctuation L'^2, L' being the r.m.s. lift, was thus written as

$$L'^2 = a^2 \int_{-\lambda}^{\lambda} \int_{-\lambda}^{\lambda} \overline{(p_1 - p_2)_\xi (p_1 - p_2)_\eta} \cos\xi \cos\eta \, d\xi \, d\eta, \tag{A 1}$$

where $a\,(= \frac{1}{2}d)$ is the radius of a circular cylinder and λ, ξ and η denote small angles measured from the diametral line $\theta = 90°$. Without any loss of generality, p_1 can be chosen as the surface-pressure fluctuation in the vicinity of $\theta = 90°$ and p_2 as that in the vicinity of $\theta = 270°$. The angle λ will be taken to be so small that the cosines in the integrand of (A 1) do not differ much from unity.

Equation (A 1) can be expanded in the form

$$L'^2/a^2 \simeq \underbrace{\int_{-\lambda}^{\lambda} \int_{-\lambda}^{\lambda} \overline{p_{1\xi} p_{1\eta}} \, d\xi \, d\eta}_{[\mathrm{I}]} - \underbrace{\int_{-\lambda}^{\lambda} \int_{-\lambda}^{\lambda} \overline{p_{1\xi} p_{2\eta}} \, d\xi \, d\eta}_{[\mathrm{II}]}$$

$$- \underbrace{\int_{-\lambda}^{\lambda} \int_{-\lambda}^{\lambda} \overline{p_{2\xi} p_{1\eta}} \, d\xi \, d\eta}_{[\mathrm{III}]} + \underbrace{\int_{-\lambda}^{\lambda} \int_{-\lambda}^{\lambda} \overline{p_{2\xi} p_{2\eta}} \, d\xi \, d\eta}_{[\mathrm{IV}]}.$$

Since the pressure fluctuations in the vicinity of $\theta = 90°$ are dominated by the vortex shedding from the cylinder, it may be reasonable to assume that $p_{1\xi}$ and $p_{1\eta}$ are well-correlated, i.e.

$$\overline{p_{1\xi} p_{1\eta}} \simeq (p_{1\xi}'^2 p_{1\eta}'^2)^{\frac{1}{2}}.$$

The r.m.s. pressure fluctuation in the neighbourhood of $\theta = 90°$ can be regarded as a slowly-varying function of θ (see figure 6). Then the term [I] was approximated by

$$[\mathrm{I}] = (2\lambda)^2 p_1'^2.$$

By the same reasoning, the term [IV] becomes

$$[\mathrm{IV}] = (2\lambda)^2 p_2'^2 = (2\lambda)^2 p_1'^2.$$

The correlations $\overline{p_{1\xi} p_{2\eta}}$ and $\overline{p_{2\xi} p_{1\eta}}$ should be approximately equal and, as will be seen in figure 8, are slowly-varying functions of α near $\alpha = 90°$. Accordingly one has

$$[\mathrm{II}] + [\mathrm{III}] = 2(2\lambda)^2 \overline{p_1 p_2}.$$

If the r.m.s. lift coefficient C_{L}' of a circular cylinder is assumed to be equal to

$$L'/[\tfrac{1}{2}\rho U_\infty^2 (2\lambda a)],$$

one finally obtains

$$C_{\mathrm{L}}' = (p_1'^2 + p_2'^2 - 2\overline{p_1 p_2})^{\frac{1}{2}} / [\tfrac{1}{2}\rho U_\infty^2]$$

$$= 2^{\frac{1}{2}} \frac{p_1'}{(\frac{1}{2})\rho U_\infty^2} (1 - C_{p_1 p_2})^{\frac{1}{2}}.$$

REFERENCES

ALLEN, H. J. & VINCENTI, W. G. 1944 Wall interference in a two-dimensional wind tunnel, with consideration of the effect of compressibility. *N.A.C.A. Rep.* no. 782.

BATHAM, J. P. 1973 Pressure distributions on circular cylinders at critical Reynolds numbers. *J. Fluid Mech.* **57**, 209–228.

BEARMAN, P. W. 1968 The flow around a circular cylinder in the critical Reynolds number regime. *N.P.L. Aero Rep.* 1257.

BEARMAN, P. W. 1971 An investigation of the forces on flat plates normal to a turbulent flow. *J. Fluid Mech.* **46**, 177–198.

BEARMAN, P. W. 1980 Bluff body flows applicable to vehicle aerodynamics. *Trans. A.S.M.E.* I, *J. Fluids Engng* **102**, 265–274.

BRUUN, H. H. & DAVIES, P. O. A. L. 1975 An experimental investigation of the unsteady pressure forces on a circular cylinder in a turbulent cross flow. *J. Sound Vib.* **40**, 535–559.

DURBIN, P. A. & HUNT, J. C. R. 1979 Fluctuating surface pressures on bluff structures in turbulent winds: Further theory and comparison with experiment. *Proc. 5th Int. Conf. on Wind Engng.*

DURBIN, P. A. & HUNT, J. C. R. 1980 On surface pressure fluctuations beneath turbulent flow round bluff bodies. *J. Fluid Mech.* **100**, 161–184.

FAGE, A. & WARSAP, J. H. 1929 The effects of turbulence and surface roughness on the drag of a circular cylinder. *A.R.C. R. & M.* no. 1283.

GERRARD, J. H. 1965 A disturbance-sensitive Reynolds number range of the flow past a circular cylinder. *J. Fluid Mech.* **22**, 187–196.

HUMPHRIES, W. & VINCENT, J. H. 1976 Near wake properties of axisymmetric bluff body flows. *Appl. Sci. Res.* **32**, 649–669.

KO, S. C. & GRAF, W. H. 1972 Drag coefficient of cylinders in turbulent flows. *Proc. A.S.C.E.* HY5, 897–912.

MODI, V. J. & EL-SHERBINY, S. 1977 Wall confinement effects on bluff bodies in turbulent flows. In *Proc. 4th Int. Conf. on Wind Effects on Buildings and Structures* (ed. K. J. Eaton), pp. 121–132. Cambridge University Press.

MORISHITA, T. & NOMURA, M. 1968 Effect of free-stream turbulence on local heat and mass transfer from circular cylinders in cross flow. *Rep. Ship Res. Inst.* no. 5, 1–27.

ROSHKO, A. 1961 Experiments on the flow past a circular cylinder at very high Reynolds number. *J. Fluid Mech.* **10**, 345–356.

SAKATA, I. 1981 Surface-pressure fluctuations on the surface of a circular cylinder of finite height attached to a rough plane surface. Ph.D. thesis, Faculty of Engineering, Hokkaido University.

SURRY, D. 1972 Some effects of intense turbulence on the aerodynamics of a circular cylinder at subcritical Reynolds number. *J. Fluid Mech.* **52**, 543–563.

TAYLOR, G. I. 1936 Statistical theory of turbulence. V – Effect of turbulence on boundary layer. Theoretical consideration of relationship between scale of turbulence and critical resistance of spheres. *Proc. R. Soc. Lond.* A **156**, 307–317.